Characterization of $G\alpha_s$ and $G\alpha_{olf}$ activation by catechol and non-catechol dopamine D1 receptor agonists

Anh Minh Nguyen[1], Ana Semeano[1], Vianna Quach[1],

Asuka Inoue[2], David E. Nichols[3], Hideaki Yano[1]

[1]Department of Pharmaceutical Sciences, School of Pharmacy and Pharmaceutical Sciences, Bouvé College of Health Sciences, Center for Drug Discovery, Northeastern University, Boston Massachusetts

[2]Graduate School of Pharmaceutical Sciences, Tohoku University, Sendai, Miyagi, Japan

[3]Division of Chemical Biology and Medicinal Chemistry, Eshelman School of Pharmacy, University of North Carolina, Chapel Hill, North Carolina

Corresponding author

Hideaki Yano

h.yano@northeastern.edu

Keywords: dopamine D1 receptor, G protein subtypes, bioluminescence resonance energy transfer, biosensors, non-catechol agonists, synaptic modulation

ABSTRACT

The dopamine D1 receptor (D1R) couples to $G\alpha_s$ and $G\alpha_{olf}$ and plays a crucial role in regulating voluntary movement and other cognitive functions, making it a potential therapeutic target for several neurological and neuropsychiatric disorders, such as Parkinson's disease and schizophrenia. In the central nervous system, $G\alpha_s$ is widely expressed in the cortex and $G\alpha_{olf}$ is predominantly found in the striatum. We used two different configurations of bioluminescence resonance energy transfer (BRET) assays and a fluorescence-based cyclic AMP (cAMP) production functional assay to test a series of tetracyclic catechol (dihydrexidine, methyl-dihydrexidine, doxanthrine) and non-catechol (tavapadon, R03, R05) D1R agonists for their activity at these G proteins. We discovered that these tetracyclic catechol compounds and R03 exerted full agonism when D1R coupled to $G\alpha_s$ but partial agonism when D1R coupled to $G\alpha_{olf}$. In contrast, tavapadon acted as a full agonist at $G\alpha_{olf}$ and a partial agonist at $G\alpha_s$. The selectivity profiles of these compounds translated to their electrophysiological effects as expected. This suggested the possibility of achieving region-specific pharmacology and opened new directions for developing D1R drugs to treat relevant neurological and neuropsychiatric disorders.

INTRODUCTION

The dopamine D1 receptor (D1R) is one of the most widely expressed dopamine (DA) receptors in the mammalian central nervous system (CNS).[1] These receptors mediate the output of most dopaminergic pathways to regulate a breadth of important physiological and behavioral functions.[2,3] D1R activation has been reported to stimulate locomotor activity,[4,5] drive motivation and reward-associated behaviors,[6,7] and mediate executive functions and working memory.[8-10] Thus, D1R appears to be a promising target for drug development against several neuropsychiatric disorders, including Parkinson's Disease (PD) and Schizophrenia.

Developing selective D1R agonists has proved to be challenging. Classic selective D1R agonists usually resemble the catechol moiety of DA. Although some D1R agonists exhibited promising effects on cognitive function[11] and locomotor activity,[12] with some even advanced to clinical trials,[13,14] they were prematurely terminated due to their severe side effects, unfavorable pharmacokinetic properties, and tolerance.[14-17] Because of these issues, there is a dire need for new D1R agonists that can overcome these limitations but are equally efficacious. In recent years, a new class of D1R agonists without the catechol moiety has been discovered. Remarkably, a few ligands from this class have demonstrated antiparkinsonian effects, encouraging pharmacokinetic profiles, and limited tolerance.[18-21]. However, little is known about the pharmacological differences since the conventional catechol and novel non-catechol agonists have not been compared in various assay modalities in a systematic way.

Among the transducers that couple to D1R, two related $G\alpha_s$-subtypes, namely $G\alpha_s$ and $G\alpha_{olf}$, can be activated differentially with biased D1R agonists.[22] In terms of CNS distribution, there is a considerable contrast in the localization of the two. Specifically, $G\alpha_{olf}$ is highly segregated and enriched in the striatal regions while $G\alpha_s$ is largely missing in the striatum and expressed in other areas such as the cortex.[23] Selective activation of either $G\alpha_s$ or $G\alpha_{olf}$ *via* D1R has neuromodulatory effects in the cortex or striatum respectively. [22] In fact, selectively activating D1R in the medial prefrontal cortex and the striatum has been suggested to be

beneficial in treating the negative symptoms of schizophrenia and PD, respectively.[24] In this regard, D1R compounds might have the advantage of achieving region-specific pharmacology. More evidence supports the idea that receptors can assume different active conformations to exert varying degrees of action at different transducers mediated by the same receptor.[25-27] Furthermore, the G protein subtype selectivity profiles appeared to be translatable to the electrophysiological events and behavior of tested animals.[22,28,29] Here, we characterize select D1R agonists for their transducer activation properties in cells, brain slices, and behavior. Our findings shed light on the conformational differences of D1R that transduce the activation of these two G proteins and the potential utility of separate targeting.

RESULTS/DISCUSSION

D1R agonists with differential efficacy at $G\alpha_s$ or $G\alpha_{olf}$ are identified in D1R-G protein engagement and activation assays.

We used receptor-Gα engagement bioluminescence resonance energy transfer (BRET), Gα-γ activation BRET, and the fluorescence-based cAMP biosensor Pink Flamindo to study three main stages of activation: (1) Conformational change within the receptor to accommodate the G protein upon agonist binding, (2) subunit rearrangement/dissociation of heterotrimeric G protein following the GTP-GDP exchange, and (3) activation of immediate signaling effector.

Inference about the full or partial agonism of one ligand is made based on a reference compound, usually the endogenous ligand of the receptor studied. For all cell-based assays, DA will be used as the reference and the efficacy of all ligands tested will be normalized to that of DA in the same condition. In addition, SKF 81297 and SKF 38393, the established full and partial D1R agonists, respectively, were used to validate the assays' sensitivity. As expected, SKF 81297 was as effective as DA in recruiting and activating both G proteins while SKF 38393 demonstrated significantly lower efficacy in both BRET configurations used **(Figure 1A, 1D, 2A, 2D).**

In this study, we investigated a series of D1R agonists with diverse structures from both catechol (dihydrexidine (DHX), methyl-dihydrexidine (m-DHX), doxanthrine (DOX))[30] and non-catechol (tavapadon (TAV), R03, R05) classes. Unlike the control compounds (i.e., DA, SKF38393, SKF81297), there was a discernible difference in the efficacy of these agonists, relative to DA, at $G\alpha_s$ and $G\alpha_{olf}$. Of the compounds tested, DHX, m-DHX, DOX, R03, and R05 exerted full agonism at recruiting $G\alpha_s$, evidenced by their comparable or significantly higher efficacy at Gαs, but acted as partial agonists in $G\alpha_{olf}$ engagement. Interestingly, TAV induced $G\alpha_{olf}$ coupling with comparable efficacy as DA but is significantly less efficacious at $G\alpha_s$ recruitment **(Figure 1 B-F, Supplementary Table 1)**. Consistent with the results obtained from

engagement BRET, the efficacy and potency of these agonists were retained when they were tested in activation BRET. TAV remained the only compound that behaved as a full agonist at $G\alpha_{olf}$ activation while the rest of the compounds showed a clear preference for activating $G\alpha_s$ over $G\alpha_{olf}$.

$G\alpha_s$–$G\alpha_{olf}$ subtype selectivity is consistently seen in G protein function at cAMP production level.

Activation of adenylyl cyclase (AC) *via* $G\alpha_s$ and $G\alpha_{olf}$ to increase cAMP is the major signaling pathway mediated by D1R. Thus, drug-induced cAMP production was studied to evaluate $G\alpha_s$ and $G\alpha_{olf}$ activities at the functional level. To monitor the intracellular cAMP dynamic, we used the red-shifted fluorescence-based biosensor Pink Flamindo.[31]

Both full and partial benzazepine catechol agonists (SKF81297 and 38393) show a consistent efficacy level in promoting cAMP production relative to DA as the G protein engagement or activation assays **(Figure 1A, 1D, 2A, 2D, 3A, 3D)**. The tetracyclic catechol compounds were equally efficacious as DA with $G\alpha_s$ but were significantly less effective with $G\alpha_{olf}$ **(Figure 3B, 3E)**. Similar to the G protein engagement and activation assays, R03 showed full and partial agonism in $G\alpha_s$- and $G\alpha_{olf}$-mediated cAMP production, respectively, while TAV behaved as a partial agonist at $G\alpha_s$ and a full agonist at $G\alpha_{olf}$ **(Figure 3C, 3F, Supplementary Table 3)**. However, in this assay, the R05-induced cAMP production E_{max} value was lower than that of DA in both G proteins. Taken together, our assays have presented a distinct profile in G-protein activation of DHX, m-DHX, DOX, TAV, and R03 at two highly homologous transducers, $G\alpha_s$ and $G\alpha_{olf}$, suggesting the possibility of developing compounds that selectively target one subtype.

Pharmacological profiles for β-arrestin 1 and 2 recruitment are distinct from G protein engagement.

β-arrestin-mediated GPCR internalization is a well-characterized major signaling event.[32] In addition, β-arrestin also acts as a scaffold to recruit components of other signaling pathways independent of G-proteins.[33] We used a BRET assay to study β-arrestin recruitment by these D1R agonists. As β-arrestin 1 and β-arrestin 2 are widely expressed in the CNS, we evaluated their activity at both subtypes relative to DA. SKF 38393 showed minimal recruitment of both β-arrestin 1 and 2 (22% and 28%, **Supplementary Table 4**). SKF 81297 was significantly less efficacious than DA in recruiting β-arrestin 1 and 2 (44% and 82%, **Supplementary Figure 1A, 1D, Supplementary Table 4**). Thus, notably, these benzazepine catechol compounds show G-protein bias as reported previously.[34]

With the exception of m-DHX at β-arrestin 1 recruitment (70%), the tetracyclic catechol compounds demonstrated a high level of β-arrestin recruitment for both subtypes. Compared to their efficacy at $G\alpha_s$ engagement BRET assay, DHX, m-DHX, and DOX appeared to be balanced agonists at these two transducers **(Supplementary Figure 1B, 1E)**. In contrast, the efficacy of the non-catechol compounds at β-arrestin 1 and 2 recruitment was significantly lower than that of DA. Cross-comparison with their E_{max} values at $G\alpha_s$ coupling revealed a clear bias for G-protein engagement of TAV, R03, and R05.

The β-arrestin-mediated GPCR internalization accounts for developing drug tolerance.[35] The high efficacy at β-arrestin recruitment of DHX, m-DHX, and DOX might explain the rapid tolerance usually seen with tetracyclic catechol D1R agonists.[16] On the other hand, the low β-arrestin recruitment of TAV could be one of the reasons for the improved tolerability of this compound.[19]

αN swap in $G\alpha_{olf}$ chimera partially mimics $G\alpha_s$ activity.

Recent cryo-EM structure studies suggested the receptor-G-protein interacting domains that contribute to the G protein subtype selectivity among different dopamine receptors.[36,37] Of the domains involved at the interface, the intracellular loop 2 (ICL2) of D1R appeared to play a crucial role in this selectivity and was within interacting distance with the αN domain of the G protein. Previously, by substituting 6 amino acids in the αN helix of $G\alpha_{olf}$ (ERLAYK) with the $G\alpha_s$ equivalent residues (DKQVYR), referred to as $G\alpha_{olf/s}$ αN, we were able to partially restore the $G\alpha_s$ selectivity of DHX in engagement BRET.[22] Here, we used the untagged $G\alpha_{olf/s}$ αN and monitored the effect of this substitution at the functional level. Compared to their effects in wildtype (WT) $G\alpha_s$ and $G\alpha_{olf}$, SKF 81297 and SKF 38393 retained their relative efficacy and potency in cAMP production in $G\alpha_{olf}$ αN **(Figure 4A)**. However, there is a clear difference in the efficacy of the other compounds when tested with the αN chimera. The tetracyclic catechol compounds (DHX, m-DHX, and DOX) significantly increased the cAMP production compared to their performance in WT $G\alpha_{olf}$, approaching the level seen in $G\alpha_s$ **(Figure 4B, Supplementary Figure 2B)**.

The effect of this substitution appeared to be more profound in the non-catechol compounds. We noticed the same trend in R03 where the efficacy in $G\alpha_{olf}$ αN was significantly enhanced from their E_{max} in WT $G\alpha_{olf}$. Strikingly, R03 efficacy in $G\alpha_{olf}$ αN was comparable to that in WT $G\alpha_s$. TAV was the only $G\alpha_{olf}$-selective compound in this set. When tested with $G\alpha_{olf}$ αN, TAV was significantly less efficacious in producing cAMP than it was in WT $G\alpha_{olf}$. In addition, TAV efficacy in $G\alpha_{olf}$ αN was not different from that of $G\alpha_s$ **(Figure 4C, Supplementary Figure 2C)**.

Notably, while the substitution significantly altered the efficacy of these compounds trending toward $G\alpha_s$, their potency remained unchanged from WT $G\alpha_{olf}$ **(Supplementary Table 3)**, suggesting that other domains might also contribute to the $G\alpha_s$-$G\alpha_{olf}$ subtype selectivity as there are less homologous domains yet to be investigated.

D1R-mediated enhancement of pathway-specific synaptic events is seen with varied efficacy levels.

Based on the distinct distribution of $G\alpha_s$ and $G\alpha_{olf}$ in the CNS, $G\alpha_s$-selective D1R agonists are expected to exert higher efficacy in modulating cortex-related electrophysiological events whereas compounds that induce better $G\alpha_{olf}$ coupling may preferentially modulate events that are associated with the striatum. The thalamus is one of the major sources of glutamate input to the cortex whereby it triggers cortical excitatory post-synaptic current (EPSC) via N-methyl-D-aspartate receptors (NMDAR). As D1R has been reported to potentiate the EPSC in the mPFC, recording EPSCs from the cortical pyramidal cells in the presence of D1R agonists may reveal NMDAR potentiation by D1R.[38-40] On the other hand, activation of D1Rs at either axons or synaptic terminals of striatal medium spiny neurons (MSN) has been reported to presynaptically facilitate the SNr inhibitory post-synaptic current (IPSC).[41-43] Thus, the IPSC recording of D1R-expressing MSN afferents in the SNr can evaluate D1R pharmacology with the degree of enhanced response.[44,45]

Here, we combined optical stimulation of channelrhodopsin-2 (ChR2)[46] and whole-cell voltage clamp on mouse brain slices to investigate D1R agonists' effects on synaptic transmission in the thalamocortical and striatonigral projections specifically. AAV5-hSyn-hChR2(H134R)-EYFP was stereotaxically injected into the mediodorsal thalamus of *Drd1a*-tdTomato BAC transgenic mice for the expression in the thalamocortical pathway. In turn, the virus was injected in the dorsal lateral striatum of WT mice for the striatonigral pathway. Three weeks post-surgery, ChR2 was successfully expressed, evidenced by the strong expression of yellow fluorescence in the cortex **(Figure 5A)** or the SNr **(Figure 5D)**. D1R-expressing pyramidal cells in mPFC elicited an EPSC upon blue LED light stimulation. When the slices were perfused with 1 μM SKF 81297, the EPSC peak amplitude significantly increased (113.4% of baseline, $p<0.01$). The same results were observed when the slices were perfused with 1 μM

DHX (113.1% of baseline, $p<0.05$). However, perfusing 1 μM tavapadon did not enhance the cortical EPSC amplitude **(Figure 5B, 5C)**.

Photostimulation of the MSN GABAergic afferent in the SNr elicited an IPSC that was markedly enhanced by 1 μM SKF 81297 (123.3% of baseline, $p<0.01$). In contrast to its effect in the mPFC, 1 μM tavapadon significantly potentiated the IPSC in the SNr (123.1% of baseline, $p<0.05$). This effect is comparable to that seen with SKF 81297. DHX, on the other hand, failed to modulate the IPSC in the SNr **(Figure 5E, 5F)**. The recordings with DHX and TAV showed that D1R agonists that preferentially activate one G protein subtype might be able to selectively modulate the electrophysiological events in the area where that G protein is enriched, indicating that D1R region-specific pharmacology can be achieved by targeting the G-protein subtypes.

Based on our electrophysiological data, we expect that selective targeting of G protein subtype via D1R would allow modulation of the neurological and neuropsychiatric outcomes associated with that region. Specifically, cortical D1R has a significant role in regulating executive functions and working memory while striatal D1R is one of the main players in voluntary movements, reward, and motivation. Thus, region-specific D1R agonists will have great implications on developing treatments for several disorders such as cognitive deficiency and movement disorder while potentially limiting the adverse off-target effects from globally activating all the D1R in the brain.

Overall, our study suggested that the *in vitro* G protein subtype selectivity profile of D1R agonists is translatable to their physiological effects and that the current design is a reliable model to screen for compounds with different clinical significance. Through the evaluation, TAV showed a unique efficacy bias towards $G\alpha_{olf}$ while tetracyclic catechol compounds showed a $G\alpha_{s}$ efficacy bias.

MATERIALS AND METHODS

Cell-based Assays

Transfection. WT or $G\alpha_s$- and $G\alpha_{olf}$-KO HEK 293T cells (CL4) are seeded at 4 million cells per 10-cm plate and cultured in Dulbecco's modified Eagle's medium (DMEM) containing 10 % fetal bovine serum (FBS), 2 mM L-glutamine and 1 % penicillin-streptomycin at 37 °C and incubated in 5 % CO_2 – 95 % moisturized air. A constant amount of cDNA is transfected using polyethyleneimine (PEI) (1:2 w/w). For engagement BRET assays, CL4 cells are transfected with D1R-RLuc (Renilla Luciferase), $G\alpha_{ss}$154-Venus or $G\alpha_{olf}$155-Venus, β2, γ7, and RIC8B. For activation BRET assays, CL4 cells are transfected with untagged D1R, $G\alpha_{ss}$67-Venus or $G\alpha_{olf}$69-Venus, β2, γ7-L8, and RIC8B. For cAMP production assays, CL4 cells are transfected with D1R, $G\alpha_{ss}$ or $G\alpha_{olf}$ or $G\alpha_{olf}$ αN, β2, γ7, RIC8B, and Pink Flamindo (a fluorescence-based cAMP biosensor). For β-Arrestin recruitment assays, WT cells are transfected with D1R-RLuc, β-Arrestin 1-Venus or β-Arrestin 2-Venus, and GRK2. The ratio between the transfected constructs has been previously optimized for the dynamic range of the drug-induced BRET change as described previously [22].

Bioluminescence resonance energy transfer (BRET). Forty-eight hours post-transfection, cells are harvested and resuspended in potassium-based buffer (140 mM KCl, 10 mM NaCl, 1 mM $MgCl_2$, 0.1 mM KEGTA, 20 mM NaHEPES, pH 7.2) for engagement and activation BRET or phosphate-buffered saline (PBS) containing 200 μM sodium bisulfite (NaBi) for β-Arrestin recruitment assays. Cells are distributed at 100,000 cells per well in a white 96-well plate and 5 μM coelenterazine H is added. Ligands at varying concentrations are added 1 minute later. For experiments with $G\alpha_{olf}$155-Venus and $G\alpha_{olf}$69-Venus, cells are pre-incubated with 10 μg/ml digitonin for 60 minutes prior to ligand addition. Bioluminescence and fluorescence emissions are recorded at 485 and 530 nm, respectively.

cAMP production assay. Cells are prepared as described above for the BRET assay, except that they are resuspended in PBS containing 200 μM NaBi and distributed in a black 96-well plate. Plate reader is set at 540 nm excitation and 590 nm emission. For all *in vitro* experiments, dose-response curves and data analysis are done using GraphPad Prism10.

Mouse-based Assays

Stereotaxic surgery. *Drd1a*-tdTomato BAC transgenic mice are anesthetized and maintained with isoflurane/oxygen through a nose cone mounted on a stereotaxic apparatus. The scalp is opened, and two holes are drilled in the skull (-0.4 mm AP, ±0.4 mm ML, -3.5 mm DV from bregma for the thalamocortical pathway; 0 mm AP, ±2 mm ML, -3 mm DV from bregma for the nigrostriatal pathway). AP, ML, DV, which stands for anterior-posterior, medial-lateral, and dorsal-ventral, respectively, are the spatial coordinates relative to the bregma. AAV5-hSynapsin-hChannelrhodopsin 2(H134R)-EYFP (Addgene) is injected (0.5 μl/side) at 0.1 μl/min. The needle is left in place for 1 minute before being slowly removed.

Slice electrophysiology. Horizontal (for the nigrostriatal pathway) and coronal slices (for the thalamocortical pathway) at 220 μm thickness are prepared using a vibratome (VT-1000S, Leica). Mice are anesthetized and perfused with modified artificial cerebral spinal fluid (m-aCSF) containing (in mM): 92 NMDG, 20 HEPES, 25 glucose, 30 $NaHCO_3$, 1.2 NaH_2PO_4, 2.5 KCl, 5 sodium ascorbate, 3 sodium pyruvate, 2 thiourea, 10 $MgSO_4$, 0.5 $CaCl_2$, 300–310 mOsm, and pH 7.3–7.4. Slices are sectioned in cold m-aCSF, recovered at 32 °C in the same buffer saturated with carbogen for 10 min, and transferred to a holding chamber filled with carbogen-saturated aCSF (holding aCSF) containing (in mM): 92 NaCl, 20 HEPES, 25 glucose, 30 $NaHCO_3$, 1.2 NaH_2PO_4, 2.5 KCl, 5 sodium ascorbate, 3 sodium pyruvate, 2 thiourea, 1 $MgSO_4$, 2 $CaCl_2$, 300–310 mOsm, and pH 7.3–7.4. During recordings, slices are continuously perfused

at 2 ml/min with carbogen-saturated aCSF containing (in mM): 124 NaCl, 2.5 KCl, 1.25 NaH_2PO_4, 1 $MgCl_2$, 26 $NaHCO_3$, 11 glucose, 2.4 $CaCl_2$, 300–310 mOsm, and pH 7.3–7.4. The temperature of the recording chamber is maintained at 31–32 °C. Electrodes (3–5 MΩ) is backfilled with an internal solution containing (in mM): 120 mM K gluconate, 20 KCl, 0.05 EGTA, 10 HEPES, 1.5 $MgCl_2$, 2.18 Na_2 ATP, 0.38 Na GTP, 10.19 Na phosphocreatine, 280–285 mOsm, and pH 7.3–7.4. Pyramidal neurons in layer V of the mPFC and GABAergic neurons in the SNr are visually identified using IR-DIC optics with an upright microscope (Olympus). Whole-cell voltage-clamp recordings (held at resting membrane potential) are made using a MultiClamp 700B amplifier (2 kHz low-pass Bessel filter and 10 kHz digitization) with pClamp 11 software (Molecular Devices).

For ChR2 evoked responses, the thalamocortical and striatonigral terminals are activated using a 473 nm DPSS blue laser. The laser is controlled by an Optogenetics TTL Pulse Generator (Doric Lenses, Quebec, Canada). The stimulation protocol consists of 4 pulsed lights at 5 s intervals with a 2 ms pulse duration at 1 mW, followed by a 40 s pause.

AUTHOR CONTRIBUTIONS

HY designed the experiments. AMN, AS, and VQ carried out the experiments, and performed the data analysis with HY. AI provided $G\alpha_s$- and $G\alpha_{olf}$-KO HEK 293T cells. DEN provided tetracyclic catechol D1R agonists. AMN and HY prepared the initial manuscript, with contributions from all the authors in finalizing the manuscript.

COMPETING INTEREST STATEMENT

The authors declare no competing financial interests.

ACKNOWLEDGEMENTS

RO3 and RO5 compounds were provided under a Material Transfer Agreement with F. Hoffmann-La Roche LTD (Basel, Switzerland). The work was supported by Northeastern University Startup Funds and Tier1 Intramural Grant (HY).

FIGURES AND FIGURE LEGENDS

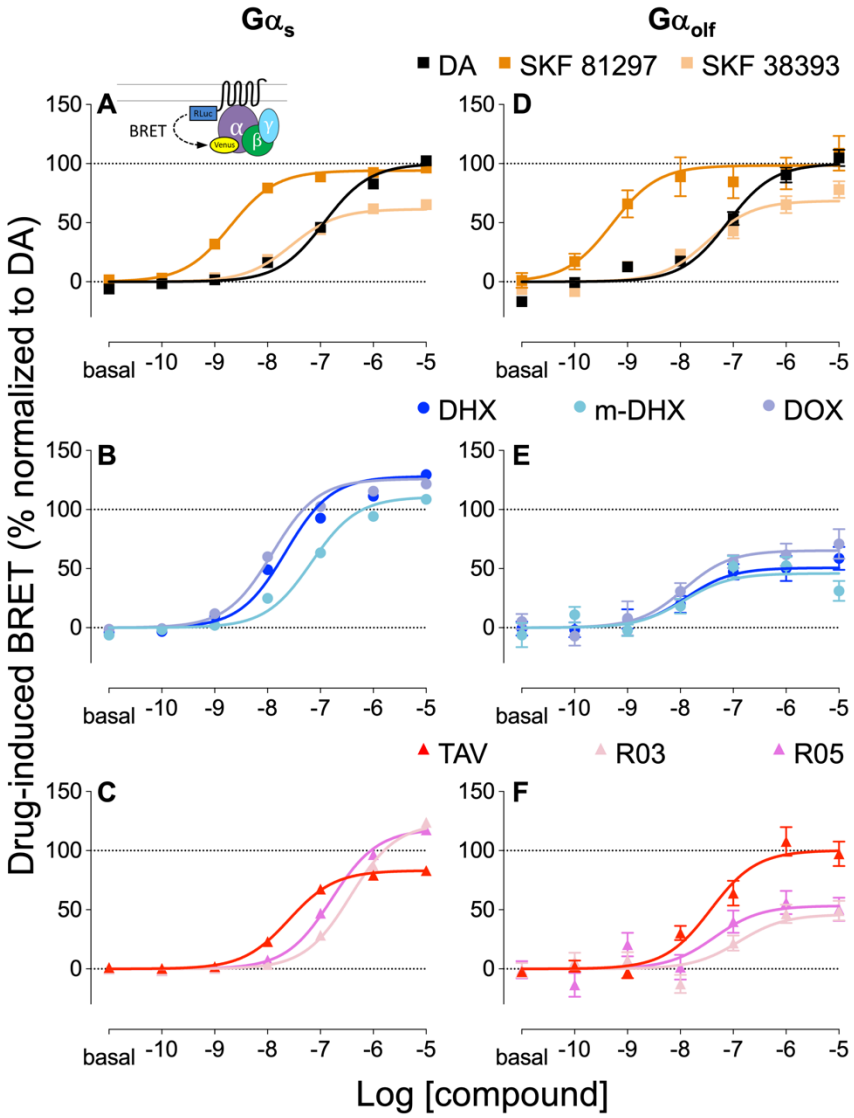

Figure 1. D1R agonist-induced D1R-Gα_s and -Gα_{olf} engagement. Drug-induced BRET ratio change between D1R-Rluc8 and Gα_s-Venus **(A, B, C)** or Gα_{olf}-Venus **(D, E, F)** in response to DA (black), SKF 81297 (dark orange), SKF 38393 (light orange) (top row), DHX (blue), m-DHX (light blue), DOX (violet) (middle row), TAV (red), R03 (pink), and R05 (magenta). Results are normalized to DA for D1R-Gα_s (**A, B, C**) and D1R-Gα_{olf} (**D, E, F**) and presented as mean ± SEM (n ≥ 5)

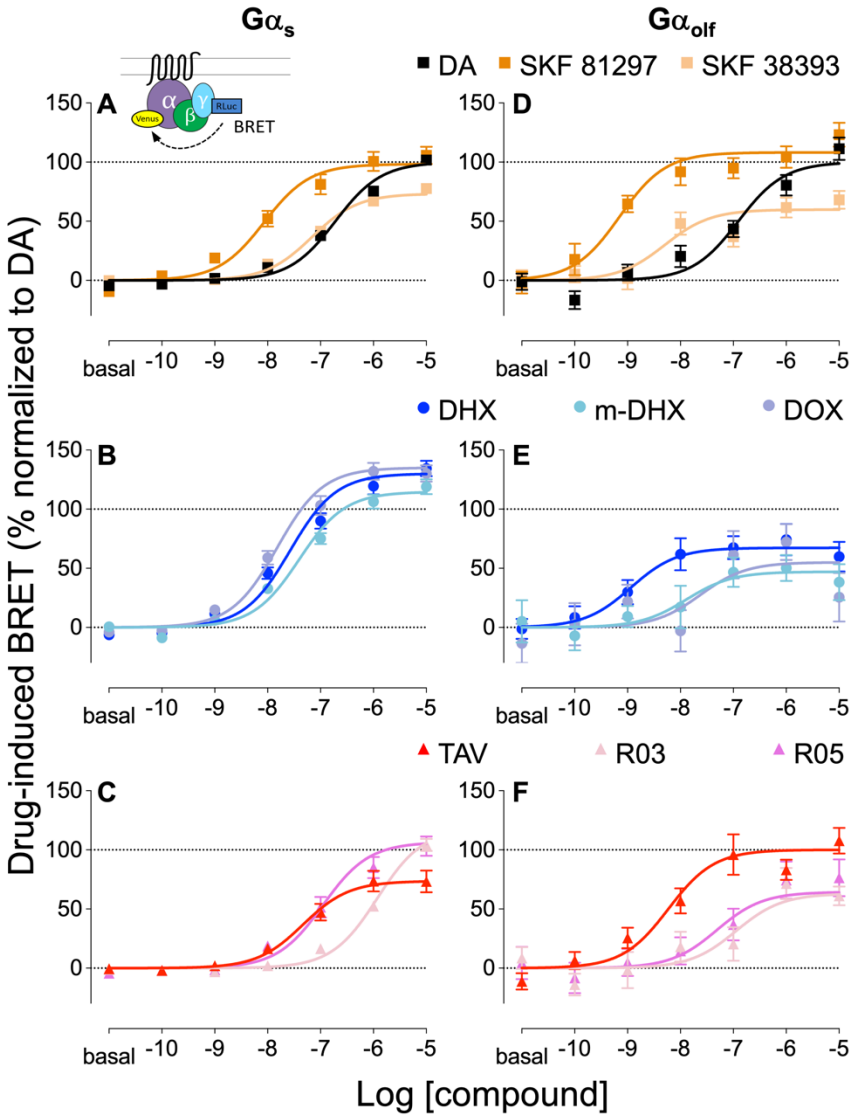

Figure 2. D1R agonist-induced D1R-Gα$_s$ and -Gα$_{olf}$ activation. Drug-induced BRET ratio change between γ7-Rluc8 and Gα$_s$-Venus **(A, B, C)** or Gα$_{olf}$-Venus **(D, E, F)** in response to DA (black), SKF 81297 (dark orange), SKF 38393 (light orange) (top row), DHX (blue), m-DHX (light blue), DOX (violet) (middle row), TAV (red), R03 (pink), and R05 (magenta). Results are normalized to DA for D1R-Gα$_s$ (**A, B, C**) and D1R-Gα$_{olf}$ (**D, E, F**) and presented as mean ± SEM (n ≥ 5)

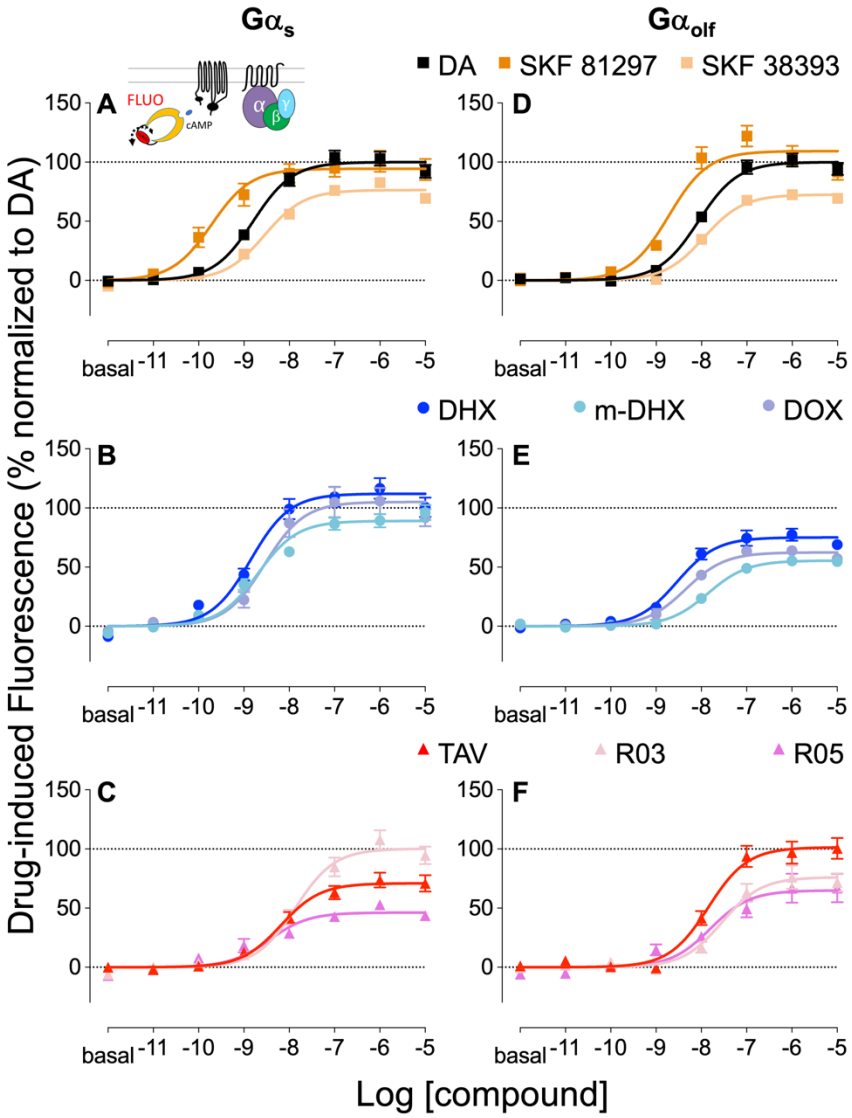

Figure 3. D1R agonist-induced cAMP production via $G\alpha_s$ and $G\alpha_{olf}$. Drug-induced fluorescence change of the cAMP biosensor Pink Flamindo in D1R-$G\alpha_s$ **(A, B, C)** or D1R-$G\alpha_{olf}$ **(D, E, F)** in response to DA (black), SKF 81297 (dark orange), SKF 38393 (light orange) (top row), DHX (blue), m-DHX (light blue), DOX (violet) (middle row), TAV (red), R03 (pink), and R05 (magenta). Results are normalized to DA for D1R-$G\alpha_s$ (**A, B, C**) and D1R-$G\alpha_{olf}$ (**D, E, F**) and presented as mean ± SEM ($n \geq 5$)

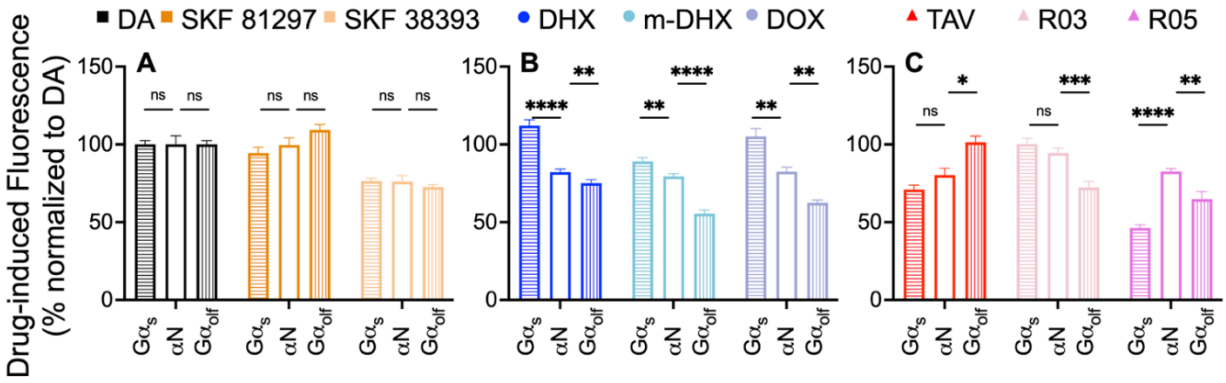

Figure 4. D1R agonist-induced cAMP production via $G\alpha_{olf/s}$ chimera. Drug-induced fluorescence change of Pink Flamindo detecting cAMP level. **A**. DA (black), SKF81297 (orange), SKF38393 (light orange), **B**. DHX (blue), m-DHX (light blue), DOX (violet), **C**. TAV (red), R03 (pink), and R05 (magenta). Fluorescence is normalized to each of DA-induced Emax values for $G\alpha_s$, $G\alpha_{olf/s}$ chimera (αN), $G\alpha_{olf}$. Results are normalized to DA for each Gα condition and presented as mean ± SEM ($n \geq 5$), one-way ANOVA, Tukey test *, **, ***, ****$p<0.05, 0.01, 0.001, 0.0001$, respectively.

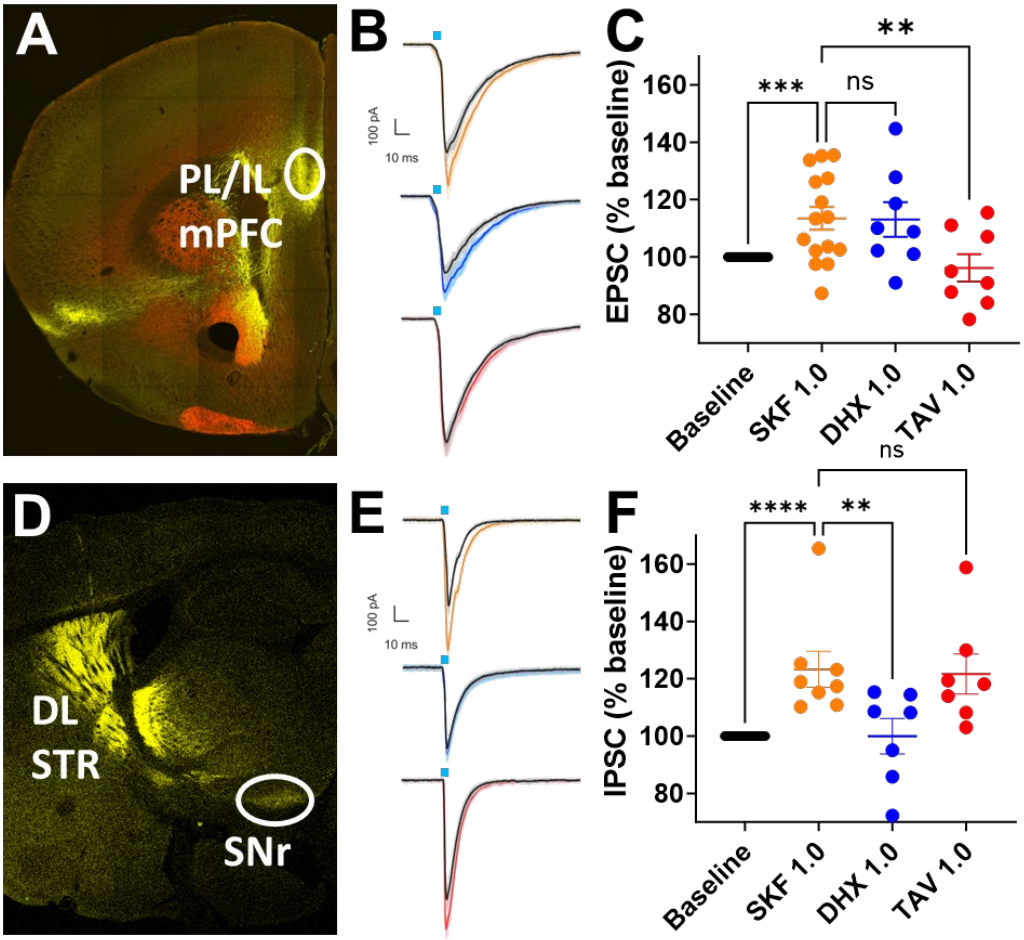

Figure 5. $G\alpha_s$ and $G\alpha_{olf}$ activities in brain slice electrophysiology. ChR2-YFP injection in the mediodorsal thalamus projecting to the prelimbic/infralimbic mPFC of D1R-tdTomato mouse **(A)** and in the dorsal striatum projecting to the SNr of WT mouse **(D).** Average trace of ChR2-elicited EPSCs in the mPFC **(B)** and IPSCs in the SNr **(E)** following 2 ms of photostimulation by blue light. Analysis of the D1R-mediated potentiation of EPSCs in the mPFC **(C)** IPSCs in the SNr **(F)**. *, **, ***, **** $p<0.05$, 0.01, 0.001, 0.0001, respectively, compared to the effect of SKF81297 using one-way ANOVA, Tukey test

REFERENCES

1. De Keyser J, Claeys A, De Backer JP, Ebinger G, Roels F, Vauquelin G. Autoradiographic localization of D1 and D2 dopamine receptors in the human brain. *Neurosci Lett*. Aug 31 1988;91(2):142-7. doi:10.1016/0304-3940(88)90758-6
2. Hegarty SV, Sullivan AM, O'Keeffe GW. Midbrain dopaminergic neurons: a review of the molecular circuitry that regulates their development. *Dev Biol*. Jul 15 2013;379(2):123-38. doi:10.1016/j.ydbio.2013.04.014
3. Beaulieu JM, Gainetdinov RR. The physiology, signaling, and pharmacology of dopamine receptors. *Pharmacol Rev*. Mar 2011;63(1):182-217. doi:10.1124/pr.110.002642
4. Waszczak BL, Martin LP, Finlay HE, Zahr N, Stellar JR. Effects of individual and concurrent stimulation of striatal D1 and D2 dopamine receptors on electrophysiological and behavioral output from rat basal ganglia. *J Pharmacol Exp Ther*. Mar 2002;300(3):850-61. doi:10.1124/jpet.300.3.850
5. Vermeulen RJ, Drukarch B, Sahadat MC, Goosen C, Wolters EC, Stoof JC. The dopamine D1 agonist SKF 81297 and the dopamine D2 agonist LY 171555 act synergistically to stimulate motor behavior of 1-methyl-4-phenyl-1,2,3,6-tetrahydropyridine-lesioned parkinsonian rhesus monkeys. *Mov Disord*. Nov 1994;9(6):664-72. doi:10.1002/mds.870090613
6. Halbout B, Marshall AT, Azimi A, et al. Mesolimbic dopamine projections mediate cue-motivated reward seeking but not reward retrieval in rats. *Elife*. 05 20 2019;8doi:10.7554/eLife.43551
7. Kravitz AV, Tye LD, Kreitzer AC. Distinct roles for direct and indirect pathway striatal neurons in reinforcement. *Nat Neurosci*. Jun 2012;15(6):816-8. doi:10.1038/nn.3100
8. Wulaer B, Kunisawa K, Tanabe M, et al. Pharmacological blockade of dopamine D1- or D2-receptor in the prefrontal cortex induces attentional impairment in the object-based attention test through different neuronal circuits in mice. *Mol Brain*. Feb 28 2021;14(1):43. doi:10.1186/s13041-021-00760-3
9. Puig MV, Miller EK. Neural Substrates of Dopamine D2 Receptor Modulated Executive Functions in the Monkey Prefrontal Cortex. *Cereb Cortex*. Sep 2015;25(9):2980-7. doi:10.1093/cercor/bhu096
10. Rinaldi A, Mandillo S, Oliverio A, Mele A. D1 and D2 receptor antagonist injections in the prefrontal cortex selectively impair spatial learning in mice. *Neuropsychopharmacology*. Feb 2007;32(2):309-19. doi:10.1038/sj.npp.1301176
11. Arnsten AF, Cai JX, Murphy BL, Goldman-Rakic PS. Dopamine D1 receptor mechanisms in the cognitive performance of young adult and aged monkeys. *Psychopharmacology (Berl)*. Oct 1994;116(2):143-51. doi:10.1007/BF02245056
12. Taylor JR, Lawrence MS, Redmond DE, et al. Dihydrexidine, a full dopamine D1 agonist, reduces MPTP-induced parkinsonism in monkeys. *Eur J Pharmacol*. Jul 09 1991;199(3):389-91. doi:10.1016/0014-2999(91)90508-n
13. Mu Q, Johnson K, Morgan PS, et al. A single 20 mg dose of the full D1 dopamine agonist dihydrexidine (DAR-0100) increases prefrontal perfusion in schizophrenia. *Schizophr Res*. Aug 2007;94(1-3):332-41. doi:10.1016/j.schres.2007.03.033
14. Blanchet PJ, Fang J, Gillespie M, et al. Effects of the full dopamine D1 receptor agonist dihydrexidine in Parkinson's disease. *Clin Neuropharmacol*. 1998 Nov-Dec 1998;21(6):339-43.
15. Rascol O, Nutt JG, Blin O, et al. Induction by dopamine D1 receptor agonist ABT-431 of dyskinesia similar to levodopa in patients with Parkinson disease. *Arch Neurol*. Feb 2001;58(2):249-54. doi:10.1001/archneur.58.2.249
16. Watts VJ, Lawler CP, Gilmore JH, Southerland SB, Nichols DE, Mailman RB. Dopamine D1 receptors: efficacy of full (dihydrexidine) vs. partial (SKF38393) agonists in primates vs. rodents. *Eur J Pharmacol*. Sep 28 1993;242(2):165-72. doi:10.1016/0014-2999(93)90076-t

17. Close SP, Marriott AS, Pay S. Failure of SKF 38393-A to relieve parkinsonian symptoms induced by 1-methyl-4-phenyl-1,2,3,6-tetrahydropyridine in the marmoset. *Br J Pharmacol*. Jun 1985;85(2):320-2. doi:10.1111/j.1476-5381.1985.tb08863.x
18. Sohur US, Gray DL, Duvvuri S, Zhang Y, Thayer K, Feng G. Phase 1 Parkinson's Disease Studies Show the Dopamine D1/D5 Agonist PF-06649751 is Safe and Well Tolerated. *Neurol Ther*. Dec 2018;7(2):307-319. doi:10.1007/s40120-018-0114-z
19. Riesenberg R, Werth J, Zhang Y, Duvvuri S, Gray D. PF-06649751 efficacy and safety in early Parkinson's disease: a randomized, placebo-controlled trial. *Ther Adv Neurol Disord*. 2020;13:1756286420911296. doi:10.1177/1756286420911296
20. Papapetropoulos S, Liu W, Duvvuri S, Thayer K, Gray DL. Evaluation of D1/D5 Partial Agonist PF-06412562 in Parkinson's Disease following Oral Administration. *Neurodegener Dis*. 2018;18(5-6):262-269. doi:10.1159/000492498
21. Young D, Popiolek M, Trapa P, et al. D1 Agonist Improved Movement of Parkinsonian Nonhuman Primates with Limited Dyskinesia Side Effects. *ACS Chem Neurosci*. 02 19 2020;11(4):560-566. doi:10.1021/acschemneuro.9b00589
22. Yano H, Cai NS, Xu M, et al. Gs- versus Golf-dependent functional selectivity mediated by the dopamine D. *Nat Commun*. 02 05 2018;9(1):486. doi:10.1038/s41467-017-02606-w
23. Hervé D. Identification of a specific assembly of the g protein golf as a critical and regulated module of dopamine and adenosine-activated cAMP pathways in the striatum. *Front Neuroanat*. 2011;5:48. doi:10.3389/fnana.2011.00048
24. Howes OD, McCutcheon R, Owen MJ, Murray RM. The Role of Genes, Stress, and Dopamine in the Development of Schizophrenia. *Biol Psychiatry*. Jan 01 2017;81(1):9-20. doi:10.1016/j.biopsych.2016.07.014
25. Onaran HO, Costa T. Agonist efficacy and allosteric models of receptor action. *Ann N Y Acad Sci*. May 30 1997;812:98-115. doi:10.1111/j.1749-6632.1997.tb48150.x
26. Urban JD, Clarke WP, von Zastrow M, et al. Functional selectivity and classical concepts of quantitative pharmacology. *J Pharmacol Exp Ther*. Jan 2007;320(1):1-13. doi:jpet.106.104463 [pii]
10.1124/jpet.106.104463
27. Yang Y. Functional Selectivity of Dopamine D. *Int J Mol Sci*. Nov 03 2021;22(21)doi:10.3390/ijms222111914
28. Von Moo E, Harpsøe K, Hauser AS, et al. Ligand-directed bias of G protein signaling at the dopamine D. *Cell Chem Biol*. 02 17 2022;29(2):226-238.e4. doi:10.1016/j.chembiol.2021.07.004
29. Bonifazi A, Yano H, Guerrero AM, et al. Novel and Potent Dopamine D. *ACS Pharmacol Transl Sci*. Feb 08 2019;2(1):52-65. doi:10.1021/acsptsci.8b00060
30. Cueva JP, Chemel BR, Juncosa JI, Lill MA, Watts VJ, Nichols DE. Analogues of doxanthrine reveal differences between the dopamine D1 receptor binding properties of chromanoisoquinolines and hexahydrobenzo[a]phenanthridines. *Eur J Med Chem*. Feb 2012;48:97-107. doi:10.1016/j.ejmech.2011.11.039
31. Harada K, Ito M, Wang X, et al. Red fluorescent protein-based cAMP indicator applicable to optogenetics and in vivo imaging. *Sci Rep*. 08 04 2017;7(1):7351. doi:10.1038/s41598-017-07820-6
32. Reiter E, Ayoub MA, Pellissier LP, et al. β-arrestin signalling and bias in hormone-responsive GPCRs. *Mol Cell Endocrinol*. Jul 05 2017;449:28-41. doi:10.1016/j.mce.2017.01.052
33. Jean-Charles PY, Kaur S, Shenoy SK. G Protein-Coupled Receptor Signaling Through β-Arrestin-Dependent Mechanisms. *J Cardiovasc Pharmacol*. Sep 2017;70(3):142-158. doi:10.1097/FJC.0000000000000482
34. Conroy JL, Free RB, Sibley DR. Identification of G protein-biased agonists that fail to recruit β-arrestin or promote internalization of the D1 dopamine receptor. *ACS Chem Neurosci*. Apr 15 2015;6(4):681-92. doi:10.1021/acschemneuro.5b00020

35. Ryman-Rasmussen JP, Griffith A, Oloff S, et al. Functional selectivity of dopamine D1 receptor agonists in regulating the fate of internalized receptors. *Neuropharmacology*. Feb 2007;52(2):562-75. doi:10.1016/j.neuropharm.2006.08.028
36. Xiao P, Yan W, Gou L, et al. Ligand recognition and allosteric regulation of DRD1-Gs signaling complexes. *Cell*. 02 18 2021;184(4):943-956.e18. doi:10.1016/j.cell.2021.01.028
37. Zhuang Y, Xu P, Mao C, et al. Structural insights into the human D1 and D2 dopamine receptor signaling complexes. *Cell*. Feb 18 2021;184(4):931-942.e18. doi:10.1016/j.cell.2021.01.027
38. Mabrouk OS, Semaan DZ, Mikelman S, Gnegy ME, Kennedy RT. Amphetamine stimulates movement through thalamocortical glutamate release. *J Neurochem*. Jan 2014;128(1):152-61. doi:10.1111/jnc.12378
39. Wang J, O'Donnell P. D(1) dopamine receptors potentiate nmda-mediated excitability increase in layer V prefrontal cortical pyramidal neurons. *Cereb Cortex*. May 2001;11(5):452-62. doi:10.1093/cercor/11.5.452
40. Chen G, Greengard P, Yan Z. Potentiation of NMDA receptor currents by dopamine D1 receptors in prefrontal cortex. *Proc Natl Acad Sci U S A*. Feb 24 2004;101(8):2596-600. doi:10.1073/pnas.0308618100
41. de Jesús Aceves J, Rueda-Orozco PE, Hernández R, et al. Dopaminergic presynaptic modulation of nigral afferents: its role in the generation of recurrent bursting in substantia nigra pars reticulata neurons. *Front Syst Neurosci*. 2011;5:6. doi:10.3389/fnsys.2011.00006
42. Timmerman W, Abercrombie ED. Amphetamine-induced release of dendritic dopamine in substantia nigra pars reticulata: D1-mediated behavioral and electrophysiological effects. *Synapse*. Aug 1996;23(4):280-91. doi:10.1002/(SICI)1098-2396(199608)23:4<280::AID-SYN6>3.0.CO;2-3
43. Chuhma N, Tanaka KF, Hen R, Rayport S. Functional connectome of the striatal medium spiny neuron. *J Neurosci*. Jan 26 2011;31(4):1183-92. doi:10.1523/JNEUROSCI.3833-10.2011
44. Radnikow G, Misgeld U. Dopamine D1 receptors facilitate GABAA synaptic currents in the rat substantia nigra pars reticulata. *J Neurosci*. Mar 15 1998;18(6):2009-16.
45. Martin LP, Waszczak BL. D1 agonist-induced excitation of substantia nigra pars reticulata neurons: mediation by D1 receptors on striatonigral terminals via a pertussis toxin-sensitive coupling pathway. *J Neurosci*. Jul 1994;14(7):4494-506.
46. Shirai F, Hayashi-Takagi A. Optogenetics: Applications in psychiatric research. *Psychiatry Clin Neurosci*. Jun 2017;71(6):363-372. doi:10.1111/pcn.12516